EESM-log-AR: An Efficient Error Model for OFDM MIMO Systems over Time-Varying Channels

Sian Jin University of Washington Seattle, WA, USA sianjin@uw.edu Sumit Roy University of Washington Seattle, WA, USA sroy@uw.edu Thomas R. Henderson University of Washington Seattle, WA, USA tomh@tomh.org

ABSTRACT

Packet-level network simulators such as ns-3 rely on efficient PHY layer abstraction represented by the packet error model for estimating link performance. For complex PHY layer designs - such as operating over frequency-selective MIMO wireless channels the runtime of the state-of-the-art error model suggested by Task Group of IEEE 802.11ax (TGax) suffers from scaling with MIMO dimensionality and bandwidth. While our prior work proposes a runtime-efficient error model in the context of Independent and Identically Distributed (IID) frequency-selective MIMO channels, here we consider the time-varying frequency-selective MIMO channels that correlate over time. Our new error model is based on the insight that our previous workflow for the IID channel scenario can be extended using autoregressive modeling to the time-correlated case. We validate the hypothesis via link simulation campaigns and show that the runtime and storage complexity of the proposed error model is low compared to existing error models.

CCS CONCEPTS

 $\bullet \ Computing \ methodologies \rightarrow \ Modeling \ methodologies; Model \ verification \ and \ validation; \\ \bullet \ Networks \rightarrow \ Wireless \ local \ area \ networks.$

KEYWORDS

Network Simulator 3 (ns-3), Time-Varying Channel, Error Model

ACM Reference Format:

Sian Jin, Sumit Roy, and Thomas R. Henderson. 2021. EESM-log-AR: An Efficient Error Model for OFDM MIMO Systems over Time-Varying Channels. In 2021 Workshop on ns-3 (WNS3 2021), June 23–24, 2021, Virtual Event, USA. ACM, New York, NY, USA, 8 pages. https://doi.org/10.1145/3460797.3460800

1 INTRODUCTION

1.1 Background

Wireless network system designers require accurate understandings of PHY layer error performance to design better higher layer network protocols. For example, the link layer error control (automatic repeat request, rate adaptation, etc.) and Transmission Control Protocol (TCP) in the wireless network can be improved

Publication rights licensed to ACM. ACM acknowledges that this contribution was authored or co-authored by an employee, contractor or affiliate of the United States government. As such, the Government retains a nonexclusive, royalty-free right to publish or reproduce this article, or to allow others to do so, for Government purposes only.

WNS3 2021, June 23–24, 2021, Virtual Event, USA

© 2021 Copyright held by the owner/author(s). Publication rights licensed to ACM. ACM ISBN 978-1-4503-9034-7/21/06...\$15.00

https://doi.org/10.1145/3460797.3460800

if the burstiness (temporal correlation) of PHY layer error is better understood [5]. Packet-level network simulators such as ns-3 thus need accurate and efficient models for representing PHY layer performance to enable trustworthy evaluation and development of upper layer protocols.

Accurate full PHY implementations that incorporate detailed symbol-level encoding/decoding to output packet error performance are slow and not suitable for use in a packet-level network simulator. As shown in Table 1, the average runtime (averaged over 10 trials, as the runtime is very stable on a computer) of the full PHY simulation is typically in the order of hours and scales with MIMO dimension and bandwidth. Error models for packetlevel wireless network simulation skip the symbol-level details and abstract the PHY layer via characterizing the instantaneous Packet Error Ratios (PERs) at the output of the PHY layer. The fundamental tension, however, is the following. The more abstract error model may only be relevant for the narrower use case for which it was derived, and may fail to accurately handle deviations (e.g. environmental or configuration changes) from that use case. But network simulation users desire error models that have a wide scope of applicability. As the error model is enhanced to extend its scope and accuracy, it becomes more complicated, and impacts packet-level simulator in terms of runtime and storage complexity. The increasingly complex components in the PHY layer, such as Orthogonal Frequency Division Multiplexing (OFDM), Multiple-Input Multiple-Output (MIMO), Frequency-Selective (FS) wireless channel, make the design of a lightweight but accurate error model quite challenging.

Table 1: Average Runtime Comparison in MATLAB: Full PHY Simulation vs. Traditional EESM L2S Mapping, 200000-packet Simulation under the Time-Varying TGax Channel at a Specific RX SNR [15]

$N_t \times N_r$	Bandwidth	Full PHY	Traditional EESM
1 × 1	20MHz	171 min	97 min
1 × 1	40MHz	201 min	126 min
4 × 2	20MHz	362 min	234 min
4×2	40MHz	544 min	320 min
8 × 2	20MHz	755 min	428 min
8 × 2	40MHz	1098 min	573 min

1.2 Taxonomy of Existing Error Models

Existing error models can be classified by their underlying channel models. Under the Independent and Identically Distributed (IID) channels where the channel gains are IID over time, the error model produces IID packet errors and the distribution of the channel gains



Figure 1: Traditional L2S Mapping for CV-TV-FS Channel

fully characterizes the channel statistics. Under the Time-Varying (TV) channels where channel gains are correlated over time, the error model produces bursty packet errors and the channel gains need to be described as random processes. Under the Continuous-Valued (CV) channels, the channel gains are continuous; under the Discrete-Valued (DV) channels, the continuous channel gains are quantized into multiple discrete states. Different channels not only produce different error statistics, but also impact the applicability and complexity of the error model.

The most general class of wireless channels is the Continuous-Valued Time-Varying Frequency-Selective (CV-TV-FS) MIMO channel. For abstracting error performance under the CV-TV-FS channel, Link-to-System (L2S) mapping [2, 8, 12, 13, 19, 25, 28] was proposed and used for the development of OFDM-based systems such as Wi-Fi, 4G LTE and 5G NR standards. We consider the L2S mapping defined by Task Group of IEEE 802.11ax (TGax) [13], namely the traditional L2S mapping in this work. As shown in Figure 1, the traditional L2S mapping requires implementing the CV-TV-FS channel model within the network simulator to generate CV-TV-FS channel matrices at runtime. The channel matrix as well as the related MIMO precoding matrix and MIMO decoding matrix are used to calculate a post-equalization (post-MIMO-processing) SNR matrix. Using a L2S mapping function, this matrix is further mapped into a single metric effective SNR. A commonly chosen L2S mapping function is the Exponential Effective SNR Mapping (EESM) L2S function [8, 19, 28]. The effective SNR summarizes all important link design features including channel frequency-selectivity, antenna correlation, the effect of MIMO precoding and decoding, modulation and coding, etc. Instantaneous PER can be predicted from the effective SNR using a PER-SNR lookup table under Additive White Gaussian Noise (AWGN) Single-Input Single-Output (SISO) channel with low complexity. Table 1 shows that the traditional L2S mapping did not scale well to account for the increased dimensionality of modern systems with high MIMO dimension and channel bandwidth. In particular, the channel generation and the post-equalization SNR matrix generation steps that involve expensive matrix computations become prohibitively runtime-expensive when the MIMO dimension and channel bandwidth increase.

In our previous work [16], we found a similar runtime complexity issue for traditional L2S mapping under Continuous-Valued Independent and Identically Distributed Frequency-Selective (CV-IID-FS) channels. Based on our observation that the distribution of the natural logarithm of the EESM based effective SNR can be well modeled by a class of 4-parameter Skew Generalized Normal (SGN) distribution, we devised EESM-log-SGN model shown in Figure 2 to bypass the runtime-expensive matrix computation steps in traditional L2S mapping and directly model the distribution of the effective SNR. The EESM-log-SGN model has been shown to be

efficient for obtaining link error for OFDM/Orthogonal Frequency-Division Multiple Access (OFDMA) MIMO/Multi-User (MU)-MIMO systems over CV-IID-FS channels (e.g., TGax channels) with high accuracy and low computational complexity. This is now the state-of-the-art error model in ns-3 having substituted for the previous YANS model [18] that is designed for OFDM SISO systems over AWGN channels. However, our previous work [16] focused on the CV-IID-FS channel case, rather than the time-correlated CV-TV-FS channel found more often in practice. In ns-3, the error model for the general time-correlated CV-TV-FS channels is long overdue, and we need to find a proper error model for ns-3 over such time-correlated TV channels.



Figure 2: EESM-log-SGN Model [16] for CV-IID-FS Channel

For system simulation over a time-correlated TV channel, a traditional approach to channel representation is based on quantizing the continuous channel gain into multiple discrete channel states, resulting in a time-correlated Discrete-Valued Time-Varying (DV-TV) channel. A Markov chain is used to model the state transitions and the resulting accuracy depends on the number of states in the model. Since 1960, the two-state (nominally: 'good' and 'bad' states) Markov channel model known as Gilbert-Elliott Channel (GEC) model has been widely used, whereby each state corresponds to a bit error ratio or PER [33]. The state in the GEC model transitions with memory of order 1 (i.e., each state only depends on the previous state) [33]. GEC was subsequently generalized into the Finite-State Markov Channel (FSMC) model [9, 14, 30, 31, 34], which contains D discrete states with memory order p (each state depends on the previous p states) and is still widely used today. More pertinent starting point to this work is wideband OFDM system evaluation over a frequency selective (DV-TV-FS) channel, for which [10] combined the L2S mapping approach with the FSMC model. Specifically, [10] quantizes the range of the effective SNR into multiple states and uses the FSMC model to directly characterize the quantized effective SNR process. In this way, [10] can efficiently simulate the error process using the quantized effective SNR process and the PER-SNR lookup table. However, the methods based on the FSMC model suffer from two disadvantages. First, only D states of the channel gain or effective SNR are generated while the real channel gain process or effective SNR processes are continuous with a potentially wide range. Second, if D is increased to improve accuracy, the number of transition probabilities to be stored exponentially scale as $D^p(D-1)$, which is significant [33].

Another potential model simplification of the time-correlated TV channel is achieved by assuming Rayleigh/Rician fading. Under this assumption, the channel gain is complex Gaussian, and hence the channel gain process over time can be modeled as an AutoRegressive (AR) process with memory order p (namely, the AR(p) model) [3, 4, 33]. Compared to the FSMC model whose

storage complexity exponentially increases with memory order p, the AR(p) model has significantly lower storage complexity as it only requires storing p+2 parameters (linear storage complexity). The AR(p) model is typically used for the frequency-flat SISO Rayleigh/Rician fading channel whose channel gain is univariate [4, 33]. The multivariate extensions of the AR(p) model to cross-correlated Rayleigh/Rician fading FS multi-subcarrier MIMO channels was shown in [3]. This extension characterizes a vector of channel gains over M correlated MIMO channels or subcarriers, and suffers from order of M^2p storage complexity [3].

From the survey above, the state-of-the-art error model (traditional L2S mapping) under the most general CV-TV-FS channel suffers from the runtime issue shown in Table 1, and requires implementing complicated CV-TV-FS channel models. Other state-of-the-art runtime-efficient error models suffer from high storage complexity or can only work well in special channels. Under the most general CV-TV-FS channel, there is no lightweight and runtime-efficient error model that can accurately characterize the error performance in the existing literature. Thus, we are motivated to propose a new error model to reflect the CV-TV-FS channel with low computational and low storage complexity for network simulators.

1.3 Contributions

Similar to EESM-log-SGN model [16] that directly characterizes the effective SNR distribution under CV-IID-FS channels, we propose to directly characterize the effective SNR process under the general CV-TV-FS channels. We find that under EESM L2S mapping, the natural logarithm of an effective SNR process can be well characterized by an AR(p) process. Thus, we name our new model the EESMlog-AR model. The novelty of the EESM-log-AR model over the AR(p) model in [3] is that the EESM-log-AR model only requires modeling a single effective SNR process while the AR(p) model in [3] requires characterizing multiple cross-correlated channel gain processes on different subcarriers or MIMO channels. Thus, the EESM-log-AR model is much more storage-efficient. Under each PHY layer setup including the channel type, OFDM MIMO setup, Modulation and Coding Scheme (MCS), channel coding and received (RX) SNR (transmitted SNR minus path loss in dB), the EESM-log-AR model only requires storing p+2 parameters (namely the log-AR parameters) for characterizing effective SNR process as an AR(p) process. This is much lower than the FSMC model, as the number of parameters in the FSMC model in each PHY layer setup increases exponentially with memory order p, but typically slightly larger than the number of parameters in the EESM-log-SGN model (i.e., 4). After storing the log-AR parameters for each PHY layer setup, the EESM-log-AR model can generate an effective SNR process directly by taking the natural logarithm of the AR(p)process with desired log-AR parameters. This effective SNR process can be used to generate an instantaneous PER process using the PER-SNR lookup table, and the instantaneous PER process is used to further predict correlated error performance via Bernoulli trials for every packet. We show the flow chart of the EESM-log-AR model in Figure 3. As the EESM-log-AR model is based on L2S mapping and does not quantize the channel, it keeps the accuracy of the traditional L2S mapping under the general CV-TV-FS channel. Since the EESM-log-AR model directly characterizes the effective

SNR process at the receiver without needing to generate channels and calculate effective SNRs within the network simulation, its runtime is very low and is insensitive to the increase of the MIMO dimension and bandwidth. Finally, due to the direct characterization of the effective SNR process, we do not need to implement complex CV-TV-FS channels in a network simulator. These properties show the benefits of the EESM-log-AR model over existing error models.



Figure 3: Proposed EESM-log-AR Model for CV-TV-FS Channel

2 SYSTEM SETUP AND EESM L2S MAPPING

2.1 System Setup

In this work, we consider the most general CV-TV-FS channel. The channel instance is assumed to be almost invariant (e.g., TGax channel models [11]) during the transmission of each packet [25]. The time t is sampled with a fixed period T_s , and the sampled time index is denoted as l. We investigate the channel and receiver performance at $t = T_s l$, $l = 1, 2, 3, \ldots$ For studying the time-correlated channel, the sample period T_s is chosen to be several times smaller than the channel coherence time (the time duration over which two received signals have a strong correlation) T_c [32]. Noise at each receiver is assumed to be AWGN [25], whose power is the same over different subcarriers. The power of AWGN and the received signal power (transmit power minus path loss in dB) determine the RX SNR. All transmissions are assumed to be interference-free.

We consider the OFDM MIMO transmission with perfect synchronization, perfect phase tracking, and Channel State Information at the Receiver/Transmitter (CSIR/CSIT) determined from noisefree channel estimate [25]. n_{ss} spatial streams are transmitted from the desired transmitter to the receiver using the set of subcarriers \mathcal{N}_{sc} . On each subcarrier $i \in \mathcal{N}_{sc}$, the modulated n_{ss} spatial streams are then mapped into n_t transmit antennas using a $n_t \times n_{ss}$ MIMO precoding matrix $F_i[l]$ for subcarrier i and time index l. The generation of the MIMO precoding matrices $F_i[l], i \in \mathcal{N}_{sc}$ requires the knowledge of the $n_r \times n_t$ frequency-domain channel matrices $H_i[l]$, $i \in \mathcal{N}_{sc}$ (CSIT). The channel $H_i[l]$ is FS as its value varies over subcarrier i and is TV as its value varies over time index l. The desired transmitted packet is passed through the channel $H_i[l]$, $i \in \mathcal{N}_{sc}$ and arrives at the n_r receive antennas at the receiver. At subcarrier i and time index l, each receiver employs linear MIMO decoding to recover the desired signal with $n_r \times n_{ss}$ MIMO decoding matrices $W_i[l], i \in \mathcal{N}_{sc}$ using the knowledge of $H_i[l], i \in \mathcal{N}_{sc}$ (CSIR). At receiver's *i*-th subcarrier $i \in \mathcal{N}_{sc}$ and for stream $j \in \{1, 2, ..., n_{ss}\}$, the post-equalization (post-MIMOdecoding) SNR $\Gamma_{i,j}[l]$ at time index l is [13]

$$\Gamma_{i,j}[l] = \frac{P_r \left| [\mathbf{W}_i[l]]_j^* \mathbf{H}_i[l] [\mathbf{F}_i[l]]_j \right|^2}{P_r ||[\mathbf{W}_i[l]]_j^* \mathbf{H}_i[l] [\mathbf{F}_i[l]]_{-j}||^2 + \sigma_k^2 ||[\mathbf{W}_i[l]]_j||^2}, \quad (1)$$

where P_r is the received signal power at the receiver from the desired transmitter, σ^2 is the AWGN power on each subcarrier of the receiver, $[\cdot]_j$ denotes the j-th column of a matrix, $[\cdot]_{-j}$ denotes the matrix excluding its j-th column, and $||\cdot||$ is the Euclidean norm of a vector. The post-equalization SNR matrix at the receiver is defined by $\Gamma[l] \triangleq (\Gamma_{i,j})_{i \in \mathcal{N}_{sc}, 1 \leq j \leq n_{ss}}$, and is an important metric reflecting packet error performance.

In this paper, we use the simulation setup in Table 2 for all simulations. A 20MHz OFDM MIMO system with SVD MIMO precoding and MMSE MIMO decoding is considered. The CV-TV-FS MIMO channel is chosen as the TGax channel model-D with Jakes' Doppler spectrum [1] generated by MATLAB WLAN [22] and Communication [21] Toolboxes. The maximum user moving speed (0.089km/h) in the channel is chosen to be the same as the maximum environmental speed in TGax channels [29]. This implies that the channel coherence time is $T_c = 0.9788$ [32]. The sample period is chosen as $T_s = 0.250$ s because the considered channel typically does not have too significant change over 0.250s according to our simulation.

Table 2: PHY Layer Simulation Setup

IEEE 802.11ax		
MATLAB WLAN &		
Communication		
Toolboxes R2020b		
200000		
TGax channel model-D [22]		
Jakes' model [1]		
0.089km/h [29]		
$T_c = 0.978s [32]$		
$T_{\rm S} = 0.250 {\rm s}$		
LDPC		
1000		
4		
15dB		
20 MHz		
Noise-free		
Perfect		
SVD/MMSE		
$n_t \times n_r = 4 \times 2$		
$n_{ss}=2$		
Intel Core i5 CPU at 2.0GHz		

2.2 Traditional EESM L2S Mapping

We now overview traditional EESM L2S mapping [7, 8], a baseline error model under the CV-TV-FS channel and a foundation of the proposed error model. The key motivation for traditional EESM L2S mapping is mapping the post-equalization SNR matrix $\Gamma[l]$ into a single scalar called the *effective SNR* $\Gamma_{eff}[l]$ to facilitate evaluating the packet error performance in network simulation. As shown in Figure 1, the traditional EESM L2S mapping requires a channel matrix generator implemented in the network simulator to generate channel matrices $H_i[l]$, $i \in \mathcal{N}_{sc}$ for each packet transmitted at time index l. Then, the MIMO precoding matrices $F_i[l]$, $i \in \mathcal{N}_{sc}$ and MIMO decoding matrices $W_i[l]$, $i \in \mathcal{N}_{sc}$ are generated based on

the channel matrices $H_i[l]$, $i \in \mathcal{N}_{SC}$ for that packet. These matrices are used to calculate the post-equalization SNR matrix $\Gamma[l]$ given by (1). Notice that the above matrix calculations for obtaining $\Gamma[l]$ are runtime-expensive. The post-equalization SNR matrix $\Gamma[l]$ is then mapped into the effective SNR given by [12, 13, 25]

$$\Gamma_{eff}[l] = -\beta \ln \left(\frac{1}{n_{sc}} \frac{1}{n_{ss}} \sum_{i \in N_{ec}} \sum_{j=1}^{n_{ss}} \exp\left(-\frac{\Gamma_{i,j}[l]}{\beta}\right) \right), \quad (2)$$

where $n_{SC} \triangleq |\mathcal{N}_{SC}|$ is the number of subcarriers, and β is EESM L2S mapping tuning parameter that depends on PHY layer configurations (channel type, OFDM MIMO setup, MCS and channel coding). The tuning parameter β in (2) is obtained by minimizing the Mean Square Error (MSE) between the instantaneous PER-effective SNR curve for the simulated frequency-selective fading channel and the instantaneous PER-SNR curve under the AWGN-SISO channel [28]. The effective SNR $\Gamma_{eff}[l]$ is mapped into an instantaneous PER $P_{ins}[l]$ using the instantaneous PER-SNR lookup table under the AWGN-SISO channel at the specified packet length, channel coding and MCS. The instantaneous packet error state Y[l] ('1' for error and '0' for success) can be predicted from the Bernoulli trial with instantaneous PER $P_{ins}[l]$. Such an error state prediction method has high accuracy in terms of average PER and temporal error correlation, as will be shown in Figure 9 and Figure 10.

We compare the runtimes of the full PHY simulation and the traditional EESM L2S mapping in Table 1. Our simulation finds that the traditional EESM L2S mapping achieves smaller runtime than the full PHY simulation. However, the runtime of the traditional EESM L2S mapping is still very large and scales with MIMO dimension and bandwidth due to generating channel matrices, precoding matrices, MIMO decoding matrices, and post-equalization SNR matrices online. According to the survey in the Introduction, there is no lightweight, runtime-efficient, and accurate error model over the general CV-TV-FS channels. This motivates us to propose a new general error model that outperforms traditional EESM L2S mapping with respect to runtime over the CV-TV-FS channels.

3 EESM-LOG-AR MODEL

In our previous work [16], we observed that the network simulator only needs the effective SNR and its mapped instantaneous PER for characterizing OFDM MIMO link performance. Thus in [16], we sought to bypass any online individual channel generation, precoder and decoder calculation as well as post-equalization SNR matrix calculation steps, and directly model the effective SNR *distribution* for a CV-IID-FS channel. In this work, we extend such an idea to the general CV-TV-FS channel with the focus on directly modeling the effective SNR *process*. The proposed effective SNR process model is called the EESM-log-AR model. We discuss the principle, model assumption validation, error performance accuracy, and simulation runtime of the EESM-log-AR model as follows.

3.1 Modeling Effective SNR Process

Inspired by [7, 16] that find the marginal distribution of $\ln(\Gamma_{eff}[l])$ approximately follows the normal (Gaussian) distribution or SGN distribution, we directly model the random process

$$X[l] \triangleq \ln(\Gamma_{eff}[l]). \tag{3}$$

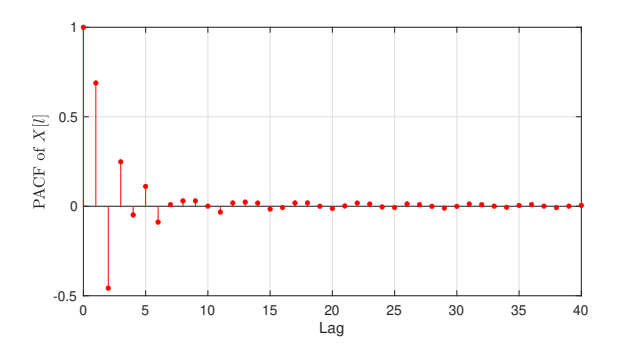


Figure 4: PACF of Effective SNR Processes under the Setup in Table 2

Since the AR(p) process is widely used in random process modeling and the marginal distribution of X[l] is approximately normal, we model the random process X[l] as the AR(p) process:

$$X[l] = c + \sum_{m=1}^{p} \phi_m X[l-m] + \epsilon[l], \tag{4}$$

where *c* is a constant, ϕ_m , m = 1, 2, ..., p are AR(p) model coefficients, and $\epsilon[l]$ is the innovation process that is assumed to be the zero-mean white Gaussian process with a constant variance σ_n^2 The AR(p) process in (4) is a Gaussian process, whose marginal distribution is Gaussian [17]. We call all the p + 2 parameters in (4) as log-AR parameters. As the effective SNR depends on the PHY layer setup including the channel type, OFDM MIMO setup, MCS, channel coding, and RX SNR (transmitted SNR minus path loss in dB), the log-AR parameters also depend on such a PHY layer setup. Notice that the log-AR parameters are insensitive to the change of packet length, because the packet length mostly impacts the instantaneous PER, not the effective SNR. The log-AR parameters under a desired PHY layer setup are generated offline and stored in the network simulator for network simulation. As X[l] is obtained from EESM L2S mapping, we call such a model the EESM-log-AR model. The flow chart of the EESM-log-AR model in a network simulator is shown in Figure 3.

The modeling of the X[l] as AR(p) process presumes X[l] is stationary. We validate this assumption using the modified Leybourne-McCabe (LMC) Test [24]. In the modified LMC test, the null hypothesis is that X[l] is a stationary AR(p) process. By our simulation, the modified LMC test fails to reject the null hypothesis with a large p-Value (> 0.05). This means that X[l] is stationary and can be modeled as an AR(p) process.

We next determine the memory order p using Partial AutoCorrelation Function (PACF). By [6], the PACF of an AR(p) process becomes 0 after lag p. From Figure 4, although we do not observe such an ideal property for X[l], it's practical to choose p to be a large enough value, such that the PACF is close to 0 afterwards. For example, from Figure 4, we choose p = 10 for the setup in Table 2.

After determining the model order p and obtaining a long sample path of X[l], we estimate the log-AR parameters c, ϕ_m , $m=1,2,\ldots,p$ and σ_p^2 using Maximum Likelihood (ML) estimation [20]. We denote the estimated log-AR parameters at RX SNR γ as $\hat{c}(\gamma)$,

Table 3: ML Estimation of Log-AR Parameters at Different RX SNRs under the Setup in Table 2 and p=10

RX SNR γ	$\hat{c}(\gamma)$	$\hat{\phi}_1(\gamma)$	$\hat{\phi}_5(\gamma)$	$\hat{\phi}_{9}(\gamma)$	$\hat{\sigma}_{10}^2(\gamma)$
12dB	0.5764	1.3454	0.3685	0.0607	0.0076
13dB	0.6525	1.2702	0.3068	0.0474	0.0085
14dB	0.7297	1.2047	0.2561	0.0370	0.0096
15dB	0.8093	1.1443	0.2128	0.0294	0.0112

 $\hat{\phi}_m(\gamma), m=1,2,\ldots,p$ and $\hat{\sigma}_p^2(\gamma)$. Table 3 shows part of the ML estimated log-AR parameters, and indicates that the estimated log-AR parameters are sensitive to the change of RX SNRs. However, storing estimated log-AR parameters for all RX SNRs for lookup at runtime is infeasible due to escalating storage complexity. As an alternative, we store log-AR parameters for a few selected RX SNRs, which are then used to interpolate these estimates for other RX SNRs. Specifically, for any RX SNR $\gamma \in [\gamma_1, \gamma_2]$, where γ_1 and γ_2 are two RX SNRs with known log-AR parameters, we can model the estimated log-AR parameters at RX SNR γ as

$$\hat{c}(\gamma) = (1 - \xi)\hat{c}(\gamma_1) + \xi\hat{c}(\gamma_2),$$

$$\hat{\phi}_m(\gamma) = (1 - \xi)\hat{\phi}_m(\gamma_1) + \xi\hat{\phi}_m(\gamma_2), \ m = 1, 2, \dots, p,$$

$$\hat{\sigma}_p^2(\gamma) = (1 - \xi)\hat{\sigma}_p^2(\gamma_1) + \xi\hat{\sigma}_p^2(\gamma_2)$$
(5)

where $\xi = \frac{\gamma - \gamma_1}{\gamma_2 - \gamma_1}$. We call the EESM-log-AR with parameters obtained using (5) as the EESM-log-AR with Linear Interpolated (LI) parameters. We can easily check the relation in (5) holds with high accuracy using the examples in Table 3. This significantly reduces the storage complexity of the EESM-log-AR model.

We plot the sample paths of X[l] obtained from EESM and the EESM-log-AR models with estimated log-AR parameters in Figure 5. From Figure 5, we can see that the EESM-log-AR model under ML parameters or LI parameters generates a process with a similar mean compared to the traditional EESM L2S mapping and does not produce outliers (very large or very small values). This shows the goodness of the EESM-log-AR model visually. For rigorous validation of the EESM-log-AR model, we present residual diagnoses and packet error performance validation in the next two subsections.

3.2 Residual Diagnoses

A standard method to validate the AR(p) model is diagnosing the residual

$$\hat{\epsilon}[l] \triangleq X[l] - \hat{c}(\gamma) - \sum_{m=1}^{p} \hat{\phi}_m(\gamma) X[l-m], \tag{6}$$

which is the estimated innovation process [6]. In the EESM-log-AR model, we assume the innovation process is white, zero-mean Gaussian, and has a constant variance. In the following, we validate these assumed properties of the innovation process. Our simulation is run at RX SNR $\gamma = 15$ dB using ML parameters and LI parameters, where the LI parameters are estimated from the ML parameters under $\gamma_1 = 14$ dB and $\gamma_2 = 16$ dB using (5).

We first test the whiteness of the residual $\hat{\epsilon}[l]$ by plotting the AutoCorrelation Function (ACF) and PACF of the residual in Figure 6. Figure 6 shows that the residual is approximately white as the ACF and PACF of residual are close to 0 at lags larger than 0.

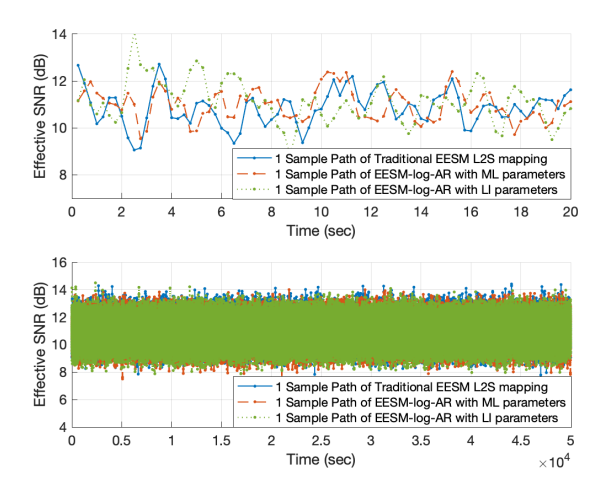


Figure 5: Sample Paths of Effective SNR Processes under the Setup in Table 2, where the Sample Period $T_s = 0.250$ s and the Coherence Time $T_c = 0.978$ s

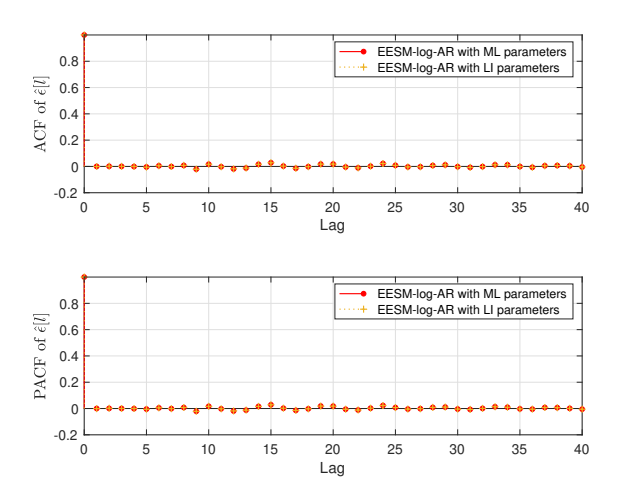


Figure 6: Residual Whiteness Test under the Setup in Table 2

We next check whether the residual $\hat{\epsilon}[l]$ follows the zero-mean Gaussian distribution. In Figure 7, we fit the empirical histogram of $\hat{\epsilon}[l]$ at 200000 continuous time instants using Gaussian distribution. The Gaussian approximation is close to zero-mean and matches the histogram of $\hat{\epsilon}[l]$. However, the skewness and kurtosis of the histogram of $\hat{\epsilon}[l]$ are 0.164 and 3.400 respectively, while the skewness and the kurtosis of a Gaussian distribution are 0 and 3 respectively. This implies that the innovation process is not exactly Gaussian, hence the marginal distribution of the X[l] is also not exactly Gaussian. In fact, in our previous work [16], we validated that the marginal distribution of the X[l] follows SGN distribution with wider ranges of skewness and kurtosis. Finding a proper innovation process that makes the marginal distribution of X[l] follow SGN distribution is non-trivial. A recent paper [27] proposes

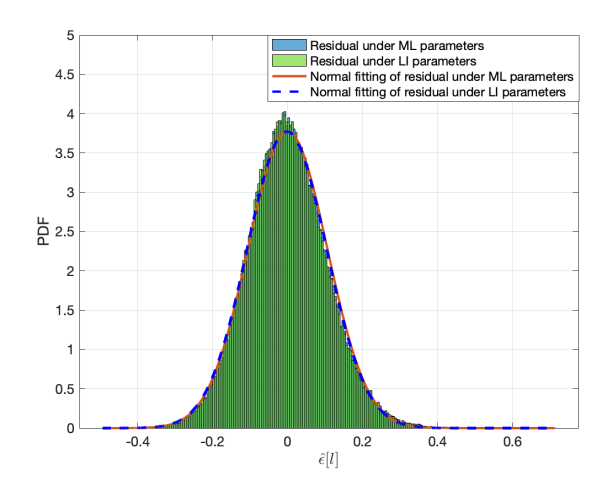


Figure 7: Residual Distribution under the Setup in Table 2

an ARSGN(p) model that modifies the AR(p) model by relaxing the white Gaussian innovation process into the IID SGN process. [27] claims that the ARSGN(p) model has higher flexibility by accommodating the skewness and kurtosis of the innovation process. We leave explorations of such model extensions for future work.

We finally check whether the residual $\hat{\epsilon}[l]$ has a constant variance by checking the whiteness of the squared residual series $\hat{\epsilon}[l]^2$ [26]. That is, if $\hat{\epsilon}[l]^2$ is white, then $\hat{\epsilon}[l]$ has a constant variance. From Figure 8, we can see that the ACF and PACF of the squared residual series are close to 0 at lag larger than 1 but have small non-zero values at lag 1. In this case, one can model X[l] as a composite AR(p) and GARCH(P, Q) process [23]. However, this can significantly increase the model complexity. In addition, from our implementation, we find that the composite AR(p) and GARCH(P, Q) modeling of X[l] can lead to higher inaccuracy in average PER prediction than the AR(p) modeling. Thus, we do not consider AR(p) and GARCH(P, Q) modeling of X[l] in this work.

This subsection validates the AR(p) modeling of $\ln(\Gamma_{eff}[I])$, an intermediate output of the EESM-log-AR error model. In the next subsection, we validate the statistics of the packet error performance, the final output of the EESM-log-AR error model that directly impacts the higher layer performance.

3.3 Packet Error Performance Validation

The effective SNR $\Gamma_{eff}[l]$ modeled in the above predicts instantaneous PER $P_{ins}[l]$ via an AWGN-SISO PER-SNR lookup table stored in the network simulator. At the output of the EESM-log-AR error model, the instantaneous packet error state Y[l] ('1' for error and '0' for success) for a packet can be predicted from the instantaneous PER $P_{ins}[l]$ via a Bernoulli trial. The first-order statistic of the packet error performance is the average PER. The average PER is the sample mean of Y[l] over multiple time instants, i.e., $\frac{1}{L}\sum_{l=1}^{L}Y[l]$, where L is the number of simulated time indices. In this work, we consider the setup in Table 2, where L=200000. The second-order statistics of the error performance are the ACF and PACF of the instantaneous error state Y[l]. The ACF of Y[l] is

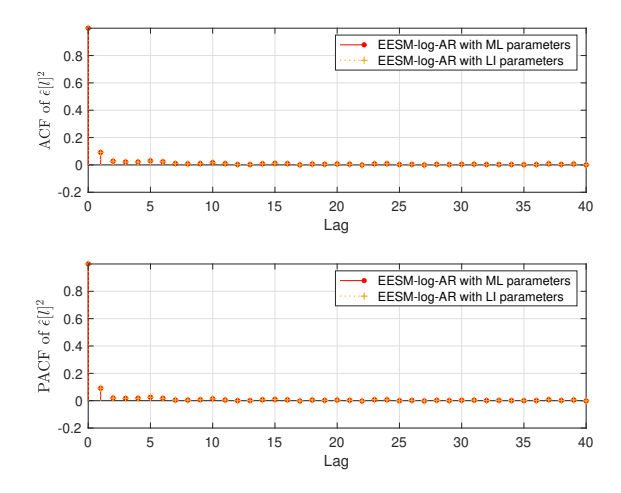


Figure 8: ACF and PACF of Squared Residual under the Setup in Table 2

widely used to validate the goodness in modeling temporal correlation of the error performance [33].

Figure 9 and Figure 10 plot the average PER, ACF, and PACF of the error performance predicted by full PHY simulation, traditional EESM L2S mapping, and EESM-log-AR error model with ML parameters and LI parameters. We find both traditional EESM L2S mapping and EESM-log-AR error model with ML parameters and LI parameters achieve very good average PER and temporal correlation prediction when compared to the most accurate full PHY simulation. Although Section 3.2 shows slight model imperfection of EESM-log-AR error model, the simulation in this part shows that the first and second order of error performance produced by the EESM-log-AR error model is very accurate. In addition, this simulation shows that the low-storage-complexity EESM-log-AR error model with LI parameters achieves almost the same first order and second order error performance as the high-storage-complexity EESM-log-AR error model with ML parameters. These results show that the EESM-log-AR error model can achieve desired first/second order error prediction performance with low-storage-complexity.

3.4 Runtime Evaluation

For traditional EESM L2S mapping or EESM-log-AR under each PHY layer setup, we need to perform the offline full PHY simulation once with runtime shown in Table 1. Table 4 shows their average runtime (averaged over 10 trials) in recursive online network simulations. We can see that the network simulation runtime of EESM-log-AR is much smaller than that of traditional EESM L2S mapping. This is because EESM-log-AR bypasses the process of generating channels and post-equalization SNRs, and directly generates effective SNR processes. Also, while the runtime of traditional EESM L2S mapping scales with MIMO dimension and bandwidth, the runtime of EESM-log-AR is insensitive to the change of the MIMO dimension and bandwidth. This is because the change of the system dimensions only changes the values of the log-AR parameters, which seldom changes the runtime of AR(p) process generation.

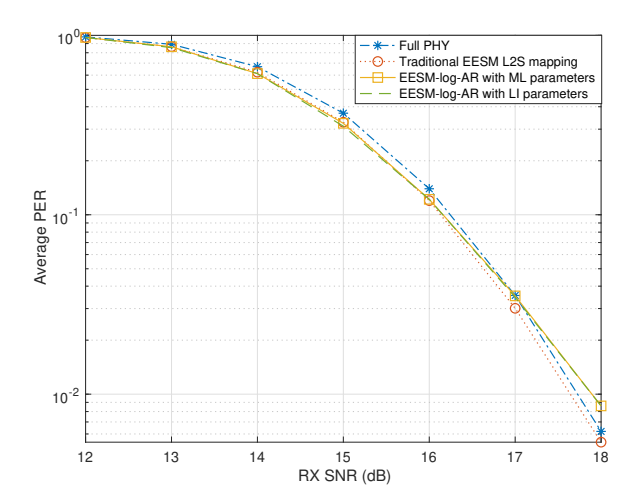


Figure 9: Comparison of Average PER under the Setup in Table 2, where the Simulated Average PER Goes Down to 10^{-2} as in Most Data Applications [29]

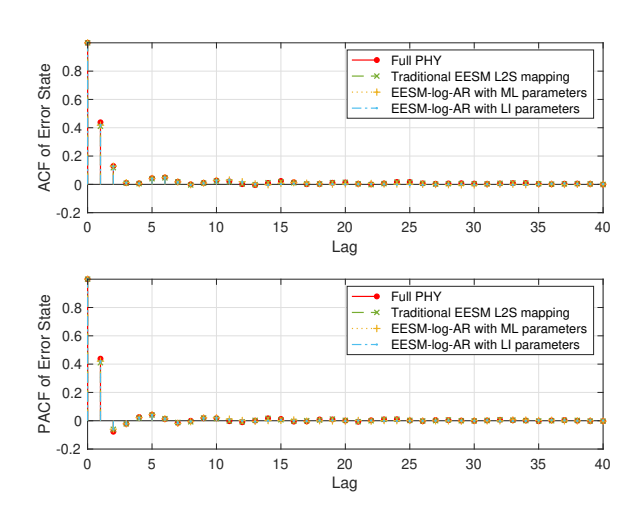


Figure 10: Comparison of ACF and PACF of Instantaneous Error State under the Setup in Table 2, where the Sample Period $T_s=0.250$ s and the Coherence Time $T_c=0.978$ s

Table 4: Average Runtime Comparison in MATLAB: EESM-log-AR vs. Traditional EESM L2S Mapping, 200000-packet Simulation under the Time-Varying TGax Channel at a Specific RX SNR [15]

$N_t \times N_r$	Bandwidth	Traditional EESM	EESM-log-AR
1 × 1	20MHz	97 min	0.4 sec
1 × 1	40MHz	126 min	0.4 sec
4×2	20MHz	234 min	0.4 sec
4×2	40MHz	320 min	0.4 sec
8 × 2	20MHz	428 min	0.4 sec
8 × 2	40MHz	573 min	0.4 sec

4 CONCLUSION AND FUTURE WORK

In this work, we showed that traditional EESM L2S mapping provides accurate packet error performance prediction under the general CV-TV-FS channel, but suffers from scaling runtime complexity with system dimension. Our previous work [16] showed a similar runtime complexity issue for the CV-IID-FS channel and dealt with this issue by proposing the EESM-log-SGN model, which bypasses the CV-IID-FS channel generation as well as post-equalization SNRs calculation and directly generates effective SNR distribution. Inspired by [16], we provided, in this work, the EESM-log-AR error model that models the effective SNR process directly. We validated the EESM-log-AR model using the modified LMC test, residual diagnoses, and error performance validation. We showed that it can predict the average PER and temporal correlation of the error performance very well, while keeping the runtime very low and insensitive to the change of system dimension. The storage complexity of the EESM-log-AR error model is low as the number of model parameters increases linearly with the memory order and the proposed LI parameter estimation further reduces the storage complexity. The EESM-log-AR error model also does not require implementing increasingly complex CV-TV-FS channels in a network simulator. These properties show that the proposed EESM-log-AR error model is a promising candidate for the error model under the general CV-TV-FS channel. The MATLAB codes related to the EESM-log-AR error model are available at [15].

We comment that our previous EESM-log-SGN model [16] is more accurate for the CV-IID-FS channel, as it accurately characterizes the marginal distribution of the logarithm of the effective SNR process using an SGN distribution (an extension of the Gaussian distribution) that can simultaneously control skewness and kurtosis. The EESM-log-AR error model proposed in this work has wider applicability as it models the error performance under the general time-correlated CV-TV-FS channel, but it lacks the accuracy in controlling the skewness and kurtosis of the marginal distribution of the the logarithm of the effective SNR process due to the Gaussian innovation assumption in the AR(p) model.

For future work, we will extend the EESM-log-AR error model to the OFDMA, MU-MIMO, and interference cases. Extending the EESM-log-AR error model to millimeter-wave channels is also a promising direction.

ACKNOWLEDGMENTS

This effort was funded in part by NSF ICE-T 1836725 and conducted in collaboration with Faisal Darbari and Colin McGuire, MathWorks Inc. The authors acknowledge their guidance on generating timevarying TGax channels with Jakes' Doppler spectrum in MATLAB.

REFERENCES

- Anritsu. 2021. Classical and Wi-Fi Doppler Spectra Comparison and Applicability. Azimuth Resource Library (2021).
- [2] Waqar Anwar, Sourav Dev, Kedar Kulkarni, Norman Franchi, and Gerhard Fettweis. 2019. On PHY Abstraction Modeling for IEEE 802.11ax based Multi-Connectivity Networks. In 2019 IEEE Wireless Communications and Networking Conference (WCNC). Marrakesh, Morocco, 1–7.
- [3] Kareem E. Baddour and Norman C. Beaulieu. 2004. Accurate Simulation of Multiple Cross-correlated Rician Fading Channels. IEEE Transactions on Communications 52, 11 (2004), 1980–1987.
- [4] Kareem E. Baddour and Norman C. Beaulieu. 2005. Autoregressive Modeling for Fading Channel Simulation. IEEE Transactions on Wireless Communications 4, 4

- (2005), 1650-1662.
- [5] Haowei Bai and Mohammed Atiquzzaman. 2003. Error Modeling Schemes for Fading Channels in Wireless Communications: A Survey. IEEE Communications Surveys and Tutorials 5, 2 (2003), 2–9.
- [6] Christopher Chatfield and Haipeng Xing. 2019. The Analysis of Time Series: An Introduction with R (7 ed.). CRC Press, Milton.
- [7] Sushruth N. Donthi and Neelesh B. Mehta. 2011. An Accurate Model for EESM and Its Application to Analysis of CQI Feedback Schemes and Scheduling in LTE. IEEE Transactions on Wireless Communications 10, 10 (2011), 3436–3448.
- [8] Jobin Francis and Neelesh B. Mehta. 2014. EESM-based Link Adaptation in Point-to-point and Multi-cell OFDM Systems: Modeling and Analysis. IEEE Transactions on Wireless Communications 13, 1 (2014), 407–417.
- [9] Robert G. Gallager. 1968. Information Theory and Reliable Communication.
- 10] IEEE TGax Group. 2013. Markov Modeling of the Channel for HEW System Level Simulations. (2013).
- [11] IEEE TGax Group. 2014. IEEE 802.11ax Channel Model Document. (2014).
- [12] IEEE TGax Group. 2014. PHY Abstraction Method Comparison. In IEEE 802.11-14/0647r2.
- [13] IEEE TGax Group. 2016. IEEE P802.11 Wireless LANs: 11ax Evaluation Methodology. (2016).
- [14] Cyril-Daniel Iskander and P. Takis Mathiopoulos. 2003. Fast Simulation of Diversity Nakagami Fading Channels Using Finite-state Markov Models. IEEE Transactions on Broadcasting 49, 3 (2003), 269–277.
- [15] Sian Jin. 2021. WNS3-2021-EESM-log-AR-code. (2021). https://github.com/sianjin/EESM-log-AR
- [16] Sian Jin, Sumit Roy, Weihua Jiang, and Thomas R. Henderson. 2020. Efficient Abstractions for Implementing TGn Channel and OFDM-MIMO Links in ns-3. In Proceedings of the 2020 Workshop on ns-3 (WNS3 2020). ACM, New York, NY, USA, 33-40.
- [17] Steven M. Kay. 2006. Intuitive Probability and Random Processes Using Matlab. Springer, New York, NY.
- [18] Mathieu Lacage and Thomas R. Henderson. 2006. Yet Another Network Simulator (WNS2 '06). ACM, New York, NY, USA, 12–22.
- [19] Sandra Lagen, Kevin Wanuga, Hussain Elkotby, Sanjay Goyal, Natale Patriciello, and Lorenza Giupponi. 2020. New Radio Physical Layer Abstraction for System-Level Simulations of 5G Networks. In *IEEE International Conference on Commu*nications (ICC). Dublin, Ireland. 1–7.
- [20] Mathworks. 2021. Estimate: Fit Autoregressive Integrated Moving Average (ARIMA) Model to Data. (2021). https://www.mathworks.com/help/econ/arima. estimate.html
- [21] Mathworks. 2021. Filter Input Signal through MIMO Multipath Fading Channel. (2021). https://www.mathworks.com/help/comm/ref/comm.mimochannel-system-object.html
- [22] Mathworks. 2021. Filter Signal through an 802.11ax Multipath Fading Channel. (2021). https://www.mathworks.com/help/wlan/ref/wlantgaxchannel-system-object.html
- [23] Mathworks. 2021. GARCH Conditional Variance Time Series Model. (2021). https://www.mathworks.com/help/econ/garch.html
- [24] Mathworks. 2021. Leybourne-McCabe Stationarity Test. (2021). https://www.mathworks.com/help/econ/lmctest.html
- [25] Mathworks. 2021. Physical Layer Abstraction for System-Level Simulation. (2021). https://www.mathworks.com/help/wlan/ug/physical-layer-abstraction-for-system-level-simulation.html
- [26] Mathworks. 2021. Residual Diagnostics. (2021). https://www.mathworks.com/ help/econ/residual-diagnostics.html
- [27] Ané Neethling, Johan Ferreira, Andriëtte Bekker, and Mehrdad Naderi. 2020. Skew Generalized Normal Innovations for the AR(p) Process Endorsing Asymmetry. Symmetry 12, 8 (2020).
- [28] Rohan Patidar, Sumit Roy, Thomas R. Henderson, and Amrutha Chandramohan. 2017. Link-to-system Mapping for ns-3 Wi-Fi OFDM Error Models. In Proceedings of the Workshop on ns-3 (WNS3 '17). ACM, New York, NY, USA, 31–38.
- [29] Eldad Perahia and Robert Stacey. 2013. Next Generation Wireless LANs: 802.11n and 802.11ac (2nd ed.). Cambridge University Press, New York, NY, USA.
- [30] Cecilio Pimentel, Tiago H. Falk, and Luciano Lisbôa. 2004. Finite-state Markov Modeling of Correlated Rician-fading Channels. IEEE Transactions on Vehicular Technology 53, 5 (2004), 1491–1501.
- [31] Qinqing Zhang and Saleem A. Kassam. 1999. Finite-state Markov Model for Rayleigh Fading Channels. IEEE Transactions on Communications 47, 11 (1999), 1688–1692.
- [32] Theodore S. Rappaport. 2002. Wireless Communications: Principles and Practice (2nd ed.). Prentice Hall.
- [33] Parastoo Sadeghi, Rodney A. Kennedy, Predrag B. Rapajic, and Ramtin Shams. 2008. Finite-state Markov Modeling of Fading Channels - a Survey of Principles and Applications. *IEEE Signal Processing Magazine* 25, 5 (2008), 57–80.
- [34] Hong Shen Wang and Nader Moayeri. 1995. Finite-state Markov Channel-A Useful Model for Radio Communication Channels. IEEE Transactions on Vehicular Technology 44, 1 (1995), 163–171.